J|A|C|S
ARTICLES
Published on Web 04/17/2002

Charge Transport through Self-Assembled Monolayers of Compounds of Interest in Molecular Electronics

Fu-Ren F. Fan,[†] Jiping Yang,[‡] Lintao Cai,[‡] David W. Price, Jr.,[‡] Shawn M. Dirk,[‡] Dmitry V. Kosynkin,[‡] Yuxing Yao,[‡] Adam M. Rawlett,[‡,§] James M. Tour,*[,‡] and Allen J. Bard*[,†]

Contribution from the Department of Chemistry and Biochemistry and Center for Nano-and Molecular Science and Technology, The University of Texas at Austin, Austin, Texas 78712, and Department of Chemistry and Center for Nanoscale Science and Technology, Rice University, Houston, Texas 77005

Received December 7, 2001

Abstract: The electrical properties of self-assembled monolayers (SAMs) on metal surfaces have been explored for a series of molecules to address the relation between the behavior of a molecule and its structure. We probed interfacial electron transfer processes, particularly those involving unoccupied states, of SAMs of thiolates or arylates on Au by using shear force-based scanning probe microscopy (SPM) combined with current−voltage ($i-V$) and current−distance ($i-d$) measurements. The $i-V$ curves of hexadecanethiol in the low bias regime were symmetric around 0 V and the current increased exponentially with V at high bias voltage. Different than hexadecanethiol, reversible peak-shaped $i-V$ characteristics were obtained for most of the nitro-based oligo(phenylene ethynylene) SAMs studied here, indicating that part of the conduction mechanism of these junctions involved resonance tunneling. These reversible peaked $i-V$ curves, often described as a negative differential resistance (NDR) effect of the junction, can be used to define a threshold tip bias, V_{TH}, for resonant conduction. We also found that for all of the SAMs studied here, the current decreased with increasing distance, d, between tip and substrate. The attenuation factor β of hexadecanethiol was high, ranging from 1.3 to 1.4 Å^{-1}, and was nearly independent of the tip bias. The β-values for nitro-based molecules were low and depended strongly on the tip bias, ranging from 0.15 Å^{-1} for tetranitro oligo(phenylene ethynylene) thiol, **VII**, to 0.50 Å^{-1} for dinitro oligo(phenylene) thiol, **VI**, at a −3.0 V tip bias. Both the V_{TH} and β values of these nitro-based SAMs were also strongly dependent on the structures of the molecules, e.g. the number of electroactive substituent groups on the central benzene, the molecular wire backbone, the anchoring linkage, and the headgroup. We also observed charge storage on nitro-based molecules. For a SAM of the dintro compound, **V**, ∼25% of charge collected in the negative scan is stored in the molecules and can be collected at positive voltages. A possible mechanism involving lateral electron hopping is proposed to explain this phenomenon.

Introduction

An understanding of how electrons flow through organic molecules is important in several areas: rationalizing electron transfer in organic and biological molecules; fabricating molecular electronic devices, such as organic light emitting devices (LEDs), memory devices, or field-effect transistors (FETs); and developing single-molecule and single-electron devices.[1] Molecular single-electron devices, including room temperature transistors, have been demonstrated recently using carbon nanotubes attached to nanoscale metal electrodes.[2] An alternative to carbon nanotubes is the use of other organic molecules, such as conjugated oligomers and aromatic molecules, in such devices. A preferred approach for the assembly of molecules into devices and their connection to the macroscopic world relies on molecular self-assembly, such as the formation of self-assembled monolayers (SAMs).[3] Covalent attachment to a metal or semiconductor surface via a suitable linking group can be easily achieved. Modern synthetic organic chemistry offers a great range of molecular structures with different properties. A challenge has been to develop reliable and fast screening methods to characterize the electronic properties of molecules and to be able to correlate the electrical behaviors of the molecules with their structures. Recent developments in device fabrication techniques and different experimental approaches

* Correspond author. E-mail: ajbard@mail.utexas.edu.
[†] The University of Texas at Austin.
[‡] Rice University.
[§] Present address: Motorola, ML34, 7700 South River Parkway, Tempe, AZ 85248.

(1) See, e.g.: (a) Kastner, M. *Phys. Today* **1993**, *46*, 24. (b) Dvoret, M. H.; Esteve, D.; Urbina, C. *Nature* **1996**, *379*, 413. (c) Tour, J. M. *Acc. Chem. Res.* **2000**, *33*, 791. (d) Jortner, J.; Ratner, M. *Molecular Electronics*; Blackwell: London, 1997.

(2) (a) Chico, L.; Crespi, V. H.; Benedict, L. X.; Louie, S. G.; Cohen, M. L. *Phys. Rev. Lett.* **1996**, *76*, 971. (b) Tans, S. J.; Devoret, M. H.; Dai, H.; Smalley, R. E.; Geerlings, L. J.; Dekker: C. *Nature* **1997**, *386*, 474.

(3) See, e.g.: (a) Ulman, A. *Chem. Rev.* **1996**, *96*, 1533. (b) Dubois, L. H.; Nuzzo, R. G. *Annu. Rev. Phys. Chem.* **1992**, *43*, 437. (c) Finklea, H. O. Electrochemistry of Organized Monolayers of Thiols and Related Molecules on Electrodes. In *Electroanalytical Chemistry*; Bard, A. J., Rubinstein, I. Eds.; Marcel Dekker: New York, Vol. 19, 1996; pp 110−335.

10.1021/ja017706t CCC: $22.00

allow single or a small group of molecules to be addressed and investigated electronically.[4]

Studies of electron transfer from a donor (**D**) to an acceptor (**A**) through a molecular bridge (**B**) for molecules in solution have provided a substantial body of information about the relation between rates of electron transfer and molecular structure. The extensive literature describing these[5] indicates that the rate of electron transfer (k_{ET}) generally depends exponentially on distance according to eq 1, in which k_0 is a

$$k_{ET} = k_0 \exp(-\beta d) \quad (1)$$

preexponential factor and β is a structure-dependent attenuation factor that describes the decay of electronic coupling between **D** and **A** as the distance separating them, d, increases. The value of the attenuation factor, β, depends strongly on the electronic structure of the molecule. β-values have been determined with several measuring techniques for different systems and range from 0.8 to 1.5 $Å^{-1}$ for alkanethiolate SAMs on Au or Hg,[5] 0.4 to 0.6 $Å^{-1}$ for oligophenylenes[6] (OPs) and 0.1 to 1.4 $Å^{-1}$ for molecules in biological systems.[7] Rates of electron transfer to a redox-active molecule in solution above SAMs of organic thiols on the surface of metal electrodes (Ag, Au, and Hg) or to one attached to the surface of a molecular tether have also been measured for films with different molecular structures. Values of β determined by this approach range from 0.9 to 1.2 $Å^{-1}$ for alkanethiol SAMs[8] and 0.06 to 0.5 $Å^{-1}$ for oligo(phenylene ethynylene)s (OPEs) and oligo(phenylene vinylene).[9]

Parallel to these approaches, solid-state metal−insulator−metal (MIM) junctions and scanning probe microscopic (SPM)[10] related techniques have also been applied to the study of ultrathin films of organic materials. Bardeen's[11] analysis of tunneling and Landauer's[12] scattering formalism have recently been used to develop models for electron transport across molecules in MIM junctions. This approach relates the conductance (g) to a transmission function, T, through eq 2,[13] where T is given by the Gamow formula (eq 3)[14] for one-dimensional tunneling, where d is the length of the molecule, W_{eff} is the effective barrier height, m is the mass of an electron, and h is Planck's constant.

$$g \propto (e^2/h)T^2 \quad (2)$$

$$T \sim \exp[-(4\pi/h)(2mW_{eff})^{1/2}d] \quad (3)$$

Since the pioneering work of Mann and Kuhn,[15] several types of MIM junctions have been fabricated. A few initial efforts have used long molecular wires across lithographically patterned proximal gold-coated probes separated by approximately 10 nm, but this approach is unreliable and not suitable for molecules shorter than the array gap. Another arrangement involves the use of the Langmuir−Blodgett technique to prepare a single molecular layer sandwiched between Al and Ti/Al contacts to form a device.[16] Other efforts employed a nanopore arrangement or mechanically controllable break junctions[17] for electrical measurements between adjustable proximal point contacts. Still others have been performed in nanopores on a structure[18] that has a metal top contact formed by vacuum evaporation, an active SAM, and a metal bottom contact. Those techniques have provided some excellent results, but the preparation of the nanostructures is very time-consuming and often results in irreproducible contacts to the molecules and shorts through the structure of interest.

To study organic ultrathin films, Majda et al. developed a MIM junction that measures tunneling current across alkanethiol SAMs sandwiched between two mercury electrodes.[19] They determined a value of $\beta = 0.8$ $Å^{-1}$ for SAMs of alkanethiols. More recently, Whitesides and co-workers have employed a similar technique to systematically study electron transport through thin organic films of a series of molecules with different structures.[20] At an applied voltage of 0.5 V, β was 0.87 ± 0.1 $Å^{-1}$ for alkanethiols, 0.61 ± 0.1 $Å^{-1}$ for oligophenylene thiols, and 0.67 ± 0.1 $Å^{-1}$ for benzylic derivatives of oligophenylene thiols. The values of β did not depend significantly on applied potential over the range of 0.1−1 V.[21] A few groups have used SPM to probe tunneling across molecules in thin organic films.[22] Conducting-probe AFM (CP-AFM)[23] appears to be especially useful in these measurements since it allows some control of

(4) See, e.g.: (a) Cygan, M, T.; Jones, L., II; Allara, D. L.; Tour, J. M.; Weiss, P. S. *J. Am. Chem. Soc.* **1998**, *120*, 2721. (b) Semaltianos, N. G. *Chem. Phys. Lett.* **2000**, *329*, 76. (c) Donhauser, Z. J.; Mantooth, B. A.; Kelly, K. F.; Bumm, L. A.; Monnell, J. D.; Stapleton, J. J.; Price, D. W., Jr.; Rawlett, A. M.; Allara, D. L.; Tour, J. M.; Weiss, P. S *Science* **2001**, *292*, 2303−2307.

(5) See, e.g.: (a) Fox, M. A. *Acc. Chem. Res.* **1999**, *32*, 201. (b) Paddon-Row: M. N. *Acc. Chem. Res.* **1994**, *27*, 18. (c) Closs, G. L.; Miller, J. R. *Science* **1988**, *240*, 440. (d) Bowler, B. E.; Raphael, A. L.; Gray, H. B. *Prog. Inorg. Chem.* **1990**, *38*, 259. (e) Fox, L. S.; Kozix, M.; Winkler, J. R.; Gray, H. B. *Science* **1990**, *247*, 1069. (f) Davis, W. B.; Svec, W. A.; Ratner, M. A.; Wasielewski, M. R. *Nature* **1998**, *396*, 60. (g) Wasielewski, M. R. *Chem. Rev.* **1992**, *92*, 435. (h) MacQueen, D. B.; Schanze, K. S. *J. Am. Chem. Soc.* **1991**, *113*, 7470.

(6) Helms, A.; Heller, D.; McLendon, G. *J. Am. Chem. Soc.* **1992**, *114*, 6227.

(7) See, e.g.: (a) Page, C. C.; Moser, C. C.; Chen, X.; Dutton, P. L. *Nature* **1999**, 47. (b) Moser, C. C.; Keske, J. M.; Warncke, K.; Farid, R. S.; Dutton, P. L. *Nature* **1992**, *355*, 796. (c) Winkler, J. R.; Di Bilio, A. J.; Farrow, N. A.; Richards, J. H.; Gray, H. B. *Pure Appl. Chem.* **1999**, *71*, 1753. (d) Kelley, S. O.; Barton, J. K. *Science* **1999**, *283*, 375. (e) Meggers, E.; Michel-Beyerle, M. E.; Giese, B. *J. Am. Chem. Soc.* **1998**, *120*, 12950. (f) Fukui, K.; Tanaka, K. *Angew. Chem., Int. Ed. Engl.* **1998**, *37*, 158.

(8) (a) Finklea, H. O.; Hanshewm D. D. *J. Am. Chem. Soc.* **1992**, *114*, 3173. (b) Becka, A. M.; Miller, C. J. *J. Phys. Chem.* **1992**, *96*, 2657. (c) Slowiski, K.; Chamberlain, R. V.; Miller, C. J.; Majda, M. *J. Am. Chem. Soc.* **1997**, *119*, 11910. (d) Chidsey, C. E. D. *Science*, **1991**, *251*, 919. (e) Smalley, J. F.; Feldberg, S. W.; Chidsey, C. E. D.; Linford, M. R.; Newton, M. D.; Liu, Y. *J. Phys. Chem.* **1995**, *99*, 13141. (f) Weber, K.; Hockett, L.; Creager, S. *J. Phys. Chem. B* **1997**, *101*, 8286.

(9) (a) Creager, S.; Yu, C. Y.; Bamdad, C.; O'Connor, S.; MacLean, T.; Lam, E.; Chong, Y.; Olsen, G. T.; Luo, J.; Gozin, M.; Kayyem, J. F. *J. Am. Chem. Soc.* **1999**, *121*, 1056. (b) Sachs, S. B.; Dudeek, S. P.; Hsung, R. P.; Sita, L. R.; Smalley, J. F.; New, M. D.; Feldberg, S. W.; Chidsey, C. E. D. *J. Am. Chem. Soc.* **1997**, *119*, 10563. (c) Sikes, H. D.; Smalley, J. F.; Dudek, S. P.; Cook, A. R.; Newton, M. D.; Chidsey, C. E. D.; Feldberg, S. W. *Science* **2001**, *291*, 1519.

(10) See, e.g.: (a) *Scanning Tunneling Microscopy and Spectroscopy*, 2nd ed.; Bonnell, D. A., Ed.; VCH: New York, 2000. (b) *Scanning Probe Microscopy: Analytical Methods*; Wiesendanger, R., Ed.; Springer-Verlag: Berlin, 1998. (c) *Scanned Probe Microscopy*; Wichramasinghe, H. K., Ed.; AIP Conference Proceedings, No. 241; American Institute of Physics: New York, 1992.

(11) Bardeen, J. *Phys. Today* **1969**, *22*, 40 and references therein.

(12) Landauer, R. *Phys. Lett. A* **1981**, *8*, 91 and references therein.

(13) Ratner, M. A.; Davis, B.; Kemp, M.; Mujica, V.; Roitberg, A.; Yaliraki, S. *Annu N.Y. Acad. Sci.* **1998**, *852*, 22.

(14) Gamow, G. *Z. Phys.* **1928**, *51*, 204.

(15) Mann, B.; Kuhn, H. *J. Appl. Phys.* **1971**, *42*, 4398.

(16) (a) Collier, C. P.; Wong, E. W.; Belohradsky, M.; Raymo, F. M.; Stoddart, J. F.; Kuekes, P. J.; Williams, R. S.; Heath, J. R. *Science* **1999**, *285*, 391. (b) Wong, E. W.; Collier, C. P.; Belohradsky, M.; Raymo, F. M.; Stoddart, J. F.; Heath, J. R. *J. Am. Chem. Soc.* **2000**, *122*, 5831.

(17) Reed, M. A.; Zhou, C.; Muller, C. J.; Burgin, T. P.; Tour, J. M. *Science* **1997**, *278*, 252.

(18) Chen, J.; Reed, M. A.; Rawlett, A. M.; Tour, J. M. *Science* **1999**, *286*, 1550.

(19) (a) Slowinski, K.; Fong, H. K. Y.; Majda, M. *J. Am. Chem. Soc.* **1981**, *103*, 7257. (b) Slowinski, K.; Majda, M. *J. Electroanal. Chem.* **2000**, *491*, 139.

(20) Rampi, M. A.; Schueller, O. J.; Whitesides, G. M. *Appl. Phys. Lett.* **1998**, *72*, 1781.

(21) Holmlin, R. E.; Haag, R.; Chabinyc, M. L.; Ismagilov, R. F.; Cohen, A. E.; Terfort, A.; Rampi, M. A.; Whiresides, G. M *J. Am. Chem. Soc.* **2001**, *123*, 5075.

Chart 1

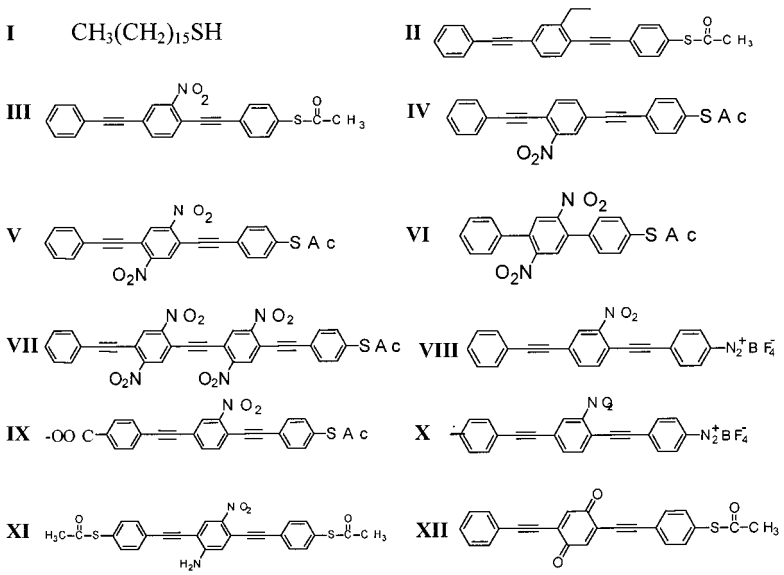

the tip location. By this technique, Frisbie[24] measured current−voltage ($i-V$) curves for SAMs of alkanethiols on Au. Weiss et al.[25] also determined β values using STM. Values of β measured by SPMs are in the range of 1.1−1.2 Å^{-1}. More recently, we reported preliminary results on the molecular electrical properties of a few SAMs of compounds of interest in molecular electronics by using a tuning fork-based scanning probe technique combined with $i-V$ measurements for rapid characterization and screening of compounds in an inert atmosphere.[26] In using a SPM technique to screen molecular monolayers, important issues are the exact location of the tip with respect to the molecules and the nature of the tip interaction with the headgroup. Of interest, in addition to β, is the appearance of peaks in the $i-V$ scan (so-called NDR phenomena) and the trapping of charge in the layer. We report here systematic studies of interfacial electron-transfer processes across SAMs by applying the same technique with extended current−distance measurements to determine the β values and the threshold voltage for electric conduction. In addition, we confirm the charge storage capability of some SAMs that occurs in addition to the usual resonant tunneling (RT) behavior and propose a mechanism involving lateral electron hopping to rationalize this observed charge trapping effect.

Experimental Section

Materials. Representative syntheses of the compounds (Chart 1) have been described elsewhere.[27] The gold substrate was prepared by cutting a single-crystal silicon wafer into 6 × 16 mm^2 pieces, then cleaned for 30 min in a hot (40 °C) fresh acidic peroxide (3:1 H_2SO_4/H_2O_2, v/v) solution. It was then rinsed with flowing distilled water, ethanol, and acetone, and dried in a flowing ultrahigh purity N_2 gas. The gold films were deposited by thermal evaporation of a 200 nm thick Au layer onto the Si sheets with a 25 nm Cr adhesion layer at a rate of 1 Å/s under a vacuum of 2×10^{-6} Torr. The gold samples were finally stored in a N_2 atmosphere. Before use, the gold substrates were cleaned in a UV/O_3 cleaner (Boekel Industries, Inc., Model 135500) for 10 min to remove any organic contamination. After ultrasonic cleaning in ethanol for 20 min, the Au substrates were rinsed with ethanol and acetone, and then dried by a stream of N_2. This procedure was confirmed to provide a clean, reproducible gold surface.[28]

Methylene chloride was distilled from calcium hydride. Tetrahydrofuran was distilled from sodium/benzophenone ketyl. All other chemicals were used as received without further purification.

SAM Preparation. SAMs were prepared by either of two reliable and reproducible methods: base-promoted or acid-promoted adsorption.[29] In the base-promoted technique, the compound (1 mg) was dissolved in a suitable solvent, e.g., ethanol, THF, or a mixture of acetone/MeOH (2:1, v/v), in a 4 mL vial to a concentration of about 0.5 mM. Concentrated NH_4OH (10 μL) was then added and the mixture was incubated for 10 min to deprotect the thiol group. Excess addition of NH_4OH (e.g., 40 μL) leads to precipitation. A 200 μL acetone/MeOH solution of 0.3 mM Cs_2CO_3 was also used for the deprotection in some cases. A clean gold substrate was then immersed into the solution at room temperature for a period of 20−24 h.

In the acid-promoted method, the compound (1 mg) was dissolved in a solvent mixture of CH_2Cl_2/MeOH (2:1 by volume) in a 4 mL vial. Concentrated H_2SO_4 (50−70 μL) was then added and the solution was incubated for 1−4 h to cause deprotection of the thiol moiety. A clean gold substrate was then immersed into the solution at room temperature

(22) See, e.g.: (a) Langlais, V. J.; Schittler, R. R.; Tang, H.; Gourdon, A.; Joachim, C.; Gimzeski, J. K. *Phys. Rev. Lett.* **2000**, *83*, 2809. (b) Datta, S.; Tian, W.; Hong, S.; Reifenger, R.; Henderson, J. I.; Kubiak, C. P. *Phys. Rev. Lett.* **1997**, *79*, 2530. (c) Zhou, S.; Liu, Y.; Xu, Y.; Hu, Z. D.; Qiu, X.; Wang, C.; Bai, C. *Chem Phys. Lett.* **1998.** *297*, 77. (d) Xue, Y.; Datta, S.; Hong, S.; Reifenger, R.; Henderson, J. I.; Kubiak, C. P. *Phys. Rev. B* **1999**, *59*, R7852. (e) Dhirani, A.-A.; Lin, P. H.; Guyot-Sionnest, P.; Zehner, R. W.; Sita, L. R. *J. Chem. Phys.* **1997**, *106*, 5249.
(23) See, e.g.: (a) Dai, H.; Wong, E. W.; Lieber, C. M. *Science* **1996**, *272*, 523. (b) Alpersion, B.; Cohen, S.; Rubinstein, I.; Hodes, G. *Phys. Rev. B* **1995**, *52*, R17017. (c) Klein, D.; McEuen, P. *Appl. Phys. Lett.* **1995**, *66*, 2478. (d) Yano, K.; Kyogaku, M.; Kuroda, R.; Shimada, Y.; Shido, S.; Matsuda, H.; Takimoto, K.; Albrecht, O.; Eguchi, K.; Nagagiri, T. *Appl. Phys. Lett.* **1996**, *68*, 188.
(24) (a) Wold, D. J.; Frisbie, C. D. *J. Am. Chem. Soc.* **2000**, *122*, 2970. (b) Kelley, T. W.; Granstrom, E. L.; Frisbie, C. D. *Adv. Mater.* **1999**, *11*, 261.
(25) Bumm, L. A.; Arnold, J. J.; Dunbar, T. D.; Allara, D. L.; Weiss, P. S. *J. Phys. Chem. B* **1999**, *103*, 8122−8127.
(26) Fan, F.-R. F.; Yang, J.; Dirk, S. M.; Price, D. W.; Kosynkin, D.; Tour, J. M.; Bard, A. J. *J. Am. Chem. Soc.* **2001**, *123*, 2454.
(27) (a) Allara, D. L.; Dunbar, T. D.; Weiss, P. S.; Bumm, L. A.; Cygan, M. T.; Tour, J. M.; Reinerth, W. A.; Yao, Y.; Kozaki, M.; Jones, L., II *Ann. N.Y. Acad. Sci.* **1998**, *852*, 349. (b) Chen, J.; Wang, W.; Reed, M. A.; Rawlett, A. M.; Price, D. W.; Tour, J. M. *Appl. Phys. Lett.* **2000**, *77*, 1224. (c) Tour, J. M.; Kozaki, M.; Seminario, J. M. *J. Am. Chem. Soc.* **1998**, *120*, 8486. (d) Sonogashira, K. In *Metal-catalyzed Cross-Coupling Reactions*; Diederich, F., Stang, P. J., Eds.; Wiley-VCH: New York, 1998; pp 203−230. (e) Tour, J. M.; Rawlett, A. M.; Kozaki, M.; Yao, Y.; Jagessar, R. C.; Dirk, S. M.; Price, D. W.; Reed, M. A.; Zhou, C.-W.; Chen, J.; Wang, W.; Campbell, I. *Chem. Eur. J.*, **2001**, *7*, 5118−5134.
(28) (a) Ron, H.; Matlis, S.; Rubinstein, I. *Langmuir* **1998**, *14*, 1116. (b) Ron, H.; Rubinstein, I. *J. Am. Chem. Soc.* **1998**, *120*, 13444.
(29) Cai, L.; Yao, Y.; Price, D. W.; Tour, J. M. *Chem. Mater.* In press.

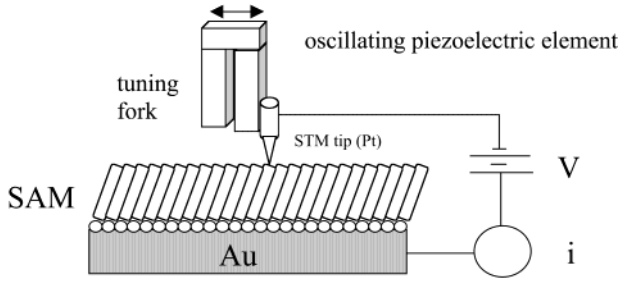

Figure 1. A systematic representation of the measurement and formation of a MIM junction with a tuning fork-based SPM tip containing a SAM on Au.

for a period of 20−24 h. All the solutions were freshly prepared, previously purged with N_2 for an oxygen-free environment, and kept in the dark during immersion. After the assembly, the samples were removed from the solutions, rinsed thoroughly with MeOH, acetone, and CH_2Cl_2, and finally blown dry with N_2.

The diazonium tetrafluoroborate salts were prepared according to previously described protocols[30] and their self-assembly was achieved on gold surfaces (prepared as described above) using the salt (1 mg) in CH_3CN (20 mL). After permitting assembly for 24 h, the gold substrate was removed and washed with CH_3CN and ethanol. Ellipsometric thicknesses were carried out under a N_2 atmosphere and were consistent (within 10−20%) with the molecular length assuming a direct aryl−gold bond.

Apparatus and Measurements. Monolayer thickness was determined with a Rudolph series 431A ellipsometer. The He−Ne laser (632.8 nm) light was incident at 70° on the sample. Measurements were carried out before and immediately after monolayer adsorption. The thickness was calculated based on a refractive index of $n_f = 1.55$, $k_f = 0$. The length of the thiolate-containing SAMs was calculated from the sulfur atom to the furthest proton for the minimum energy extended forms by molecular mechanics. The theoretical thickness was then obtained with an assumed linear Au−S−C bond angle and 0.24 nm for the Au−S bond length.

The current−voltage ($i-V$) and current−distance ($i-d$) curves were measured with a custom-built SPM[31] having a tuning fork attachment for shear-force measurement. The construction and testing of this shear force sensor followed closely the procedures reported previously by Karrai and Grober.[32] A sharpened Pt wire (diameter $\sim 100\ \mu$m), serving as the tip, was glued on the side of one of the prongs of a quartz crystal tuning fork. Such tuning forks are commercially available for operation at 32768 Hz (Digi-Key, Thief River Falls, MN)). The mechanical resonance of the fork was excited with a piezoelectric tube so that the tuning fork and the tip vibrated parallel to the sample surface. When the tip just contacted the SAM surface, the amplitude and frequency of the oscillation decreased and this point can be used to sense the presence of the surface. This allows the tip to be moved to the substrate and positioned fairly rapidly. The tip was then retracted slightly (about 20 nm) and moved to a different location on the SAM. The SPM was then operated in an STM mode. The $i-V$ curves were obtained by sweeping the potential of the tip with respect to the substrate over a desired potential range (at 6 V/s) and recording the current, as the tip approached the SAM, in small steps (1.5−3.5 Å each step). The current−distance curves were obtained by biasing the tip at a fixed potential and approaching it very slowly (at about 1 nm/s) toward the surface of the SAM and measuring the current flowing through the junction as a function of tip displacement. A schematic representation of the measurement and formation of a MIM junction with a tuning fork-based SPM tip over a SAM on Au is shown in Figure 1. The radius of the tip in contact with the SAM is roughly 5 nm at the largest distance, which corresponds to contacting about 35−100 molecules. In the discussions that follow, current direction is called "cathodic" to represent an electron flow from the tip to the SAM and "anodic" to indicate the reverse flow. All measurements were carried out at room temperature (26.5 ± 0.5 °C) under dried argon in the dark.

(30) Kosynkin, D. V.; Tour, J. M. *Org. Lett.* **2001**, *3*, 993−995.
(31) Fan, F.-R. F.; Bard, A. J. *J. Electrochem. Soc.* **1989**, *136*, 3216.
(32) (a) Karrai, K.; Grober, R. D. *Appl. Phys. Lett.* **1995**, *66*, 1842. (b) Atia W. A.; Daivs, C. C. *Appl. Phys. Lett.* **1997**, *70*, 405.

Results

High-quality SAMs could be assembled on Au based on the methods described above and were characterized by ellipsometry and electrochemical techniques; the results are reported elsewhere.[29] If not otherwise mentioned, the SAMs used here were prepared by the base-promoted chemical assembly technique.

Current−Voltage Characteristics. We measured the current that flowed across a SAM in response to changes in bias voltage while the tip approached stepwise toward the surface of a SAM on Au. Before the tip contacts the molecules in the SAM, essentially no current in excess of the noise (∼0.2 pA) flows. When a current greater than the noise level was observed, the first and several subsequent $i-V$ curves were recorded as the tip moved toward the film in 1.5−3.5 Å steps. The $i-V$ curves of each compound were taken at different locations on the same, or with different films (e.g. two or more different films for compounds **III**, **V**, and **VII**).

(a) Electrical Breakdown of Hexadecanethiol. The breakdown voltage of a SAM is manifested by an irreversible peak current flowing across the junction in response to increasing applied voltage. Figure 2 shows several first $i-V$ curves of a SAM of hexadecanethiol, **I**, for different voltage scan upper limits and at different tip positions on or in the SAM. Each $i-V$ curve was taken at a different new location, if not otherwise mentioned, and its general shape was quite reproducible. Panels A and B in Figure 2 show two typical $i-V$ curves over a range of −2 to +2 and −3 to +3 V, respectively, with the tip slightly penetrating the film. These plots show that the current was nearly symmetric about 0 V and increased exponentially at high bias voltage. This is consistent with tunneling of electrons across a MIM junction. From the current−distance relation (see eq 4), we estimate that curve 2B was taken at a distance ∼3 Å further from the substrate surface, as compared to curve 2A. As shown in Figure 2C, an increase in the upper limit of the voltage scan to −5 to +5 V, corresponding to a distance increase of ∼1.5 Å as compared to curve 2B, showed a negative current spike at ca. −4.95 V. This spike was only seen in the forward scan, with no corresponding current seen in the reverse scan to positive potentials to +5 V. Notice also that essentially no current in excess of the noise level was detected in the subsequent positive scans at the same location, indicating that the current spike is associated with an irreversible process where some type of breakdown may take place. The mechanism of this breakdown is still unclear and requires further investigation. Some $i-V$ curves showed monotonically increasing currents, even up to the saturation current of the current amplifier, 0.5 nA (not shown).

(b) Electron Transport Across Molecular Wire and Nitro-Based SAMs. Figure 3A shows the first $i-V$ curve when the tip barely touches the surface of a SAM of 2′-ethyl-4,4′-bis-(phenylethynyl)-1-benzenethiolate, **II**, on gold. The current flow through the film corresponds to the onset of conduction of the molecule and the shape of the response is different than either the tunneling behavior (exponentially monotonic increase) or

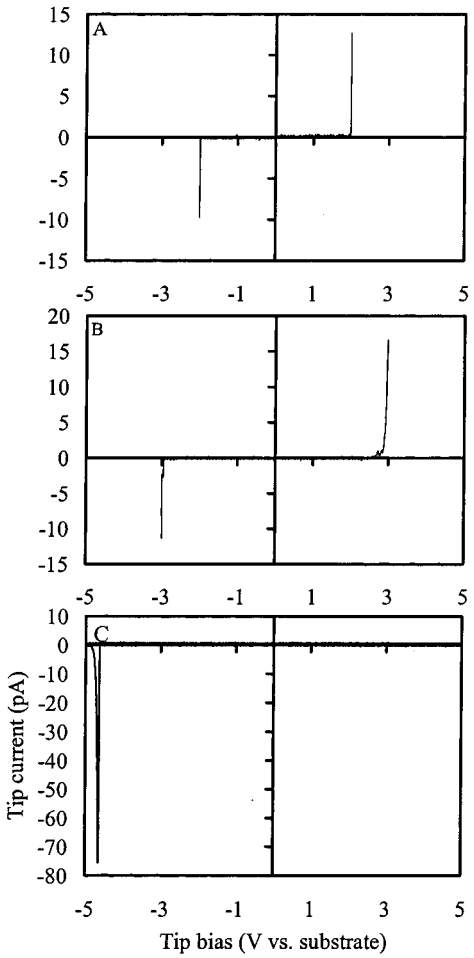

Figure 2. Three first $i-V$ curves of compound **I** for three different voltage scan upper limits: −2.0 to +2.0 V (curve A); −3.0 to +3.0 V (curve B); and −5.0 to +5.0 V (curve C). Potentials represent tip bias vs gold and all scans were taken from 0 V first toward negative bias and then to positive values.

the irreversible breakdown (no retraceable peak) seen with **I**. As shown, when the negative scan reaches about −2.8 V, a peaked current response of a few pA is observed. Notice that a similar peak is also observed at nearly the same potential in the reverse scan, although the peak height shows some variation. This indicates that it is a reversible process. We define this peak potential as the threshold tip bias (V_{TH}) for resonant conduction. As shown in Figure 3B, when the tip has been moved toward the Au surface in a small step (e.g., a 3.5 Å step), no new peaks appeared. Although the observed peak current increased substantially with decreasing tip−substrate gap, the peak potential changed much less significantly (i.e., V_{TH} was −2.65 and −2.75 V at relative distances into the film of 0 and 3.5 Å, respectively). Interestingly, a scan to positive tip bias, either initially (see Figure 3C,D) or after the scan to negative values (see Figure 3A,B), for **II** resulted in the appearance of a positive peak at about 2.9 V.

When the ethyl group at the 2′ position of the central benzene ring is substituted by an electron-accepting nitro group to yield **III**, the first V_{TH} shifted to a less negative value as compared to that for **II** (compare Figure 4A with Figure 3). As shown in Figure 4A for **III**, a pair of small but nearly retraceable peaks of ∼2 pA height were observed at ca. −2.3 V whereas **II** (Figure 3, A or B) showed the first V_{TH} at ca. −2.8 V. This $i-V$ curve

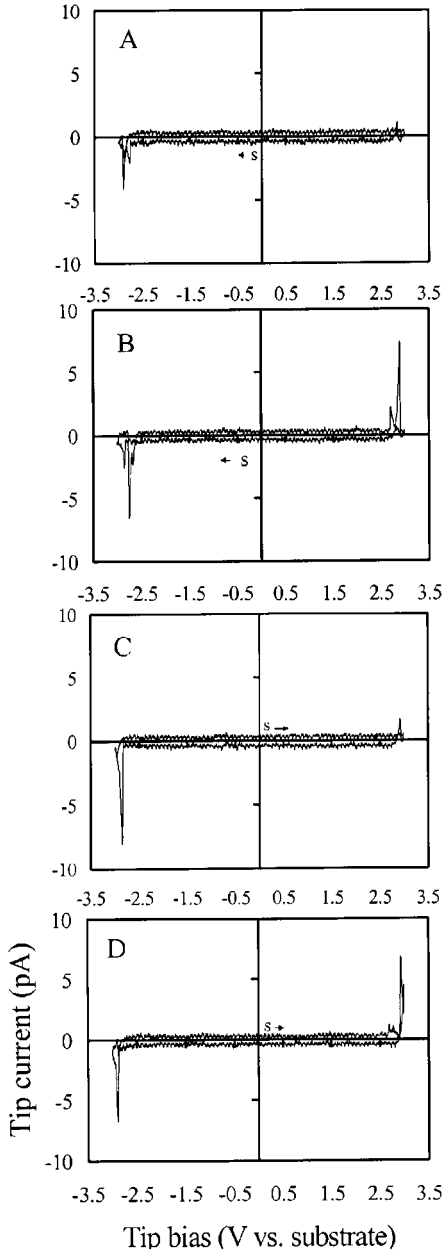

Figure 3. $i-V$ curves recorded as the tip approaches in 3.5 Å steps to the surface (from frame A to frame B for negative potential scan initially, and from frame C to frame D for positive scan initially) of a SAM of compound **II** on gold.

also clearly shows at least two current peaks in the negative bias region, which are probably related to the well-known multielectron redox activity of nitro compounds. With compound **III**, an initial scan to a positive tip bias at a fresh location did not show a peak in the voltage range of 0 to 3 V (not shown), thus the oxidation of the electroactive center in **II** takes place at a greater bias due to the presence of the nitro group. However, anodic peaks appeared after the scan to negative bias. Movement of the nitro group from position 2′ to 3′ of the central benzene ring (i.e. to form compound **IV)** shifted the first V_{TH} to a slightly more negative value as compared to **III** (see Table 1); however, it did not substantially change the shape of the $i-V$ characteristic (not shown).

The presence of two nitro groups at the central ring to form **V** further modified the $i-V$ response of the molecule. As shown

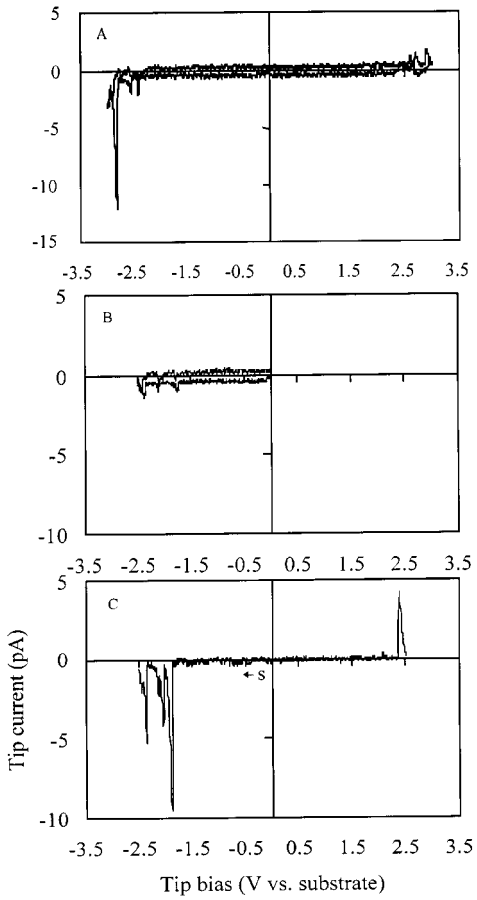

Figure 4. (A) One typical first $i-V$ curve for compound **III.** Tip voltage was scanned from 0 to the negative limit, back to 0, then to the positive limit, and finally stopped at 0 V. (B and C) Two $i-V$ curves for compound **V**. Tip bias was scanned negatively from 0 V.

in panels B and C in Figure 4, several nearly reversible peaks can clearly be identified in the negative bias region. The addition of a second nitro group to the molecule makes the electroactive center a better electron acceptor and thus shifts the first V_{TH} to a less negative value (ca. −1.8 V) as compared to **III** (ca. −2.3 V). As with compound **III**, an initial positive tip potential scan to a bias up to +3.0 V at a new location did not show a peak with **V**; however, anodic peaks appeared after the scan to negative bias. This phenomenon will be described in more detail in the section on charge storage.

It is interesting to compare the $i-V$ characteristics of the dinitro compound having an OPE backbone, i.e., **V**, with those of the compound having an OP backbone (i.e. without the triple bonds), compound **VI**. As shown in Table 1, the first negative V_{TH} of **VI** was shifted to a more negative value than that of **V**. This is probably a result of the steric-induced inter-ring twisting being greater in **VI** than in **V**, hence **VI** has more hindered electronic transport. The data obtained with these different SAMs and the V_{TH} values are summarized in Table 1. Note that the tetranitro compound, **VII**, shows at least four peaks in the range of −1.7 to −3.0 V tip bias.

(c) Effect of Anchoring Groups at the (Substrate/SAM) Interface and Headgroups at the (Tip/SAM) Interface on V_{TH}. There are contact resistances and potential drops at the interfaces between the tip and headgroup and the substrate and anchoring group, and the terminal group may also impose an internal barrier to electron transfer through the molecule. These can be important in the design of molecules with a small barrier height for charge injection (e.g. in possible molecular electronic devices). As shown in Figure 5A and Table 1, the diazonium salt, **VIII**, which probably produces a gold−aryl bond upon loss of N_2, shows a significantly less negative first V_{TH} as compared with the same compound with a thiol linkage, **III** (−1.64 vs −2.25 V). This suggests that the gold−aryl linkage has a smaller barrier for interfacial electron transfer as compared with a gold−sulfur bond.[33]

To demonstrate the effect of the headgroup at the (tip/SAM) interface on the V_{TH}, we show one of the $i-V$ curves of a COO^--terminated mono-nitro compound, **IX**, in Figure 5B (NH_4^+ as likely counterion). As shown in Table 1, **IX** shows a more negative first negative V_{TH} (ca. −2.75 V) as compared with **III**, which has an H, instead of a COO^-, as the headgroup. The substantial increase (∼0.5 eV) in the barrier height for electron injection can be mainly attributed to the blocking and electrostatic effect of the COO^- terminal group. As another example for the effect of headgroups on the electrical properties of SAMs, we show the $i-V$ curve of compound **X** in Figure 5C. **X**, like **VIII**, has a gold−aryl bond linkage at the (substrate/SAM) interface, but different than **VIII**, it has a methyl headgroup at the (tip/SAM) interface. The methyl headgroup seems to have a substantial blocking effect for electron injection from the tip to the molecule, since the first negative V_{TH} of **X** is substantially (∼0.55 V) higher than that for **VIII**. We are currently investigating systematically the effect of a series of different headgroups of the same compound and different tip materials on the $i-V$ characteristics and these results will be reported elsewhere.

(d) Electron Transport Across Other SAMs. We previously reported electrical measurements on the test aminonitro-based compound, **XI**, which has well-documented reported data. In good agreement with the results reported previously,[18] **XI** has a first negative V_{TH} at ca. −2.09 V while it shows practically no current in the voltage range as the tip potential is initially scanned to positive values (see Figure 6B). This type of peaked current response has been called a negative differential resistance (NDR) effect in the literature and the reversibility of the current flow in either negative or positive bias region suggests molecular resonant tunneling diode (MRTD) behavior. However, the peak height of the current that flows in both scan directions shows some degree of variation. To probe other related electron-withdrawing moieties, we investigated the $i-V$ characteristics of quinone-containing structures. The compound with a central quinone structure, **XII**, has the least first negative V_{TH} of the compounds listed in Table 1. As shown in Figure 6A, it has a reversible first V_{TH} at −1.58 V and an irreversible positive peak at ca. +1.7 V after the scan to negative bias. Similar to the nitro-containing SAMs, an initial positive scan of the tip bias at a fresh location did not show a peak in the voltage range from 0 to +2.0 V.

(e) Reversibility of the Negative Current Peaks and Charge Storage. We tested the reversibility of the current peak in the negative tip bias region by biasing the tip (with the STM feedback-circuit turned off) at a peak potential and approaching the tip to the surface of a SAM until a certain amount of current starts to flow through the junction. We then held the tip at a

(33) Seminario, J. M.; Zacarias, A. G.; Tour, J. M. *J. Am. Chem. Soc.* **1999**, *121*, 411−416.

Table 1. Threshold Tip Bias (V_{TH}) for Electric Conduction of Several Compounds

	negative peak voltage,[a] V				1st positive
compd	1st	2nd	3rd	4th	peak voltage,[d] V
I	~ -4.95[b]				
II	-2.79 ± 0.15				2.76 ± 0.10[e]
III	-2.25 ± 0.10	-2.82 ± 0.03			2.67 ± 0.08
IV	-2.56 ± 0.03	-2.84 ± 0.02			2.56 ± 0.07
V	-1.75 ± 0.10[c]	-2.48 ± 0.02	-2.81 ± 0.01		1.90 ± 0.10
VI	-2.24 ± 0.04	-2.58 ± 0.03	-2.82 ± 0.02		2.06 ± 0.09
VII	-1.74 ± 0.10[c]	-2.09 ± 0.03	-2.52 ± 0.02	-2.78 ± 0.04	1.89 ± 0.12
VIII	-1.64 ± 0.20	-2.05 ± 0.03			
IX	-2.75 ± 0.10				2.50 ± 0.10
X	-2.21 ± 0.15	-2.80 ± 0.08			2.50 ± 0.08
XI	-2.09 ± 0.09				1.79 ± 0.04[f]
XII	-1.58 ± 0.15				1.65 ± 0.10

[a] V_{TH} values are taken as the average of 15 to 25 $i-V$ curves for each compound (standard deviation shown). [b] Irreversible breakdown occurred. [c] Reversible but invisible sometimes in both scan directions. [d] If not otherwise mentioned, positive peaks were only observed after the tip voltage was initially scanned to the negative values first. V_{TH} values are taken as the average of 5 to 10 curves for each compound (standard deviation shown). [e] Positive tip bias scan at a location never scanned initially to a negative regime. [f] Invisible sometimes in the first positive scan at a location never scanned initially to a negative regime.

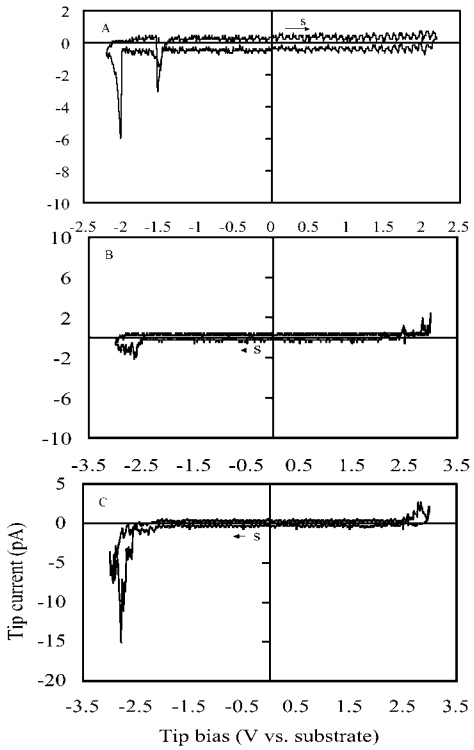

Figure 5. Three typical $i-V$ curves for compounds **VIII** (curve A), **IX** (curve B), and **X** (curve C).

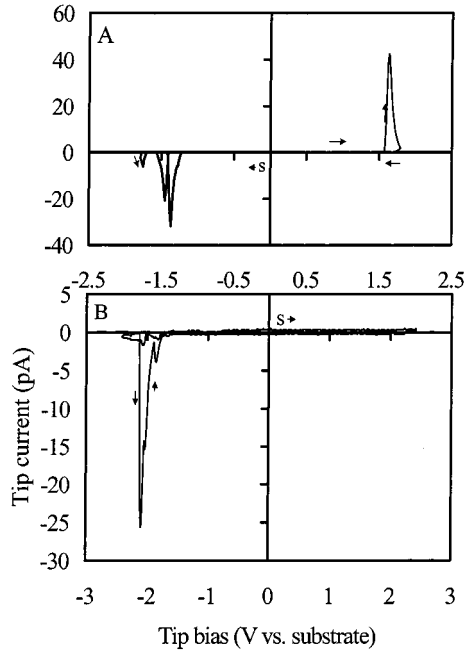

Figure 6. Typical $i-V$ curves for compounds **XII** (curve A) and **XI** (curve B). See Table 1.

constant distance from the substrate and recorded the current for a period that was greater than the time required for one complete cycle of the $i-V$ measurement (on the order of 1 s).

Figure 7 shows one typical plot of the current at a tip bias of -2.8 V for a based-promoted SAM of compound **V** as a function of time. As shown, the current fluctuated with time but did not decrease rapidly with time to the noise level as usually observed for the current peak in the $i-V$ curve. This indicates that the current peak is associated with some steady-state potential-dependent processes rather than a pure transient, time-dependent, phenomenon. It is difficult to maintain a fixed tip/substrate distance for extended time periods, however. For a longer time period, the current increased with time, probably because of the drift of the tip toward the substrate surface. This potential-dependent, rather than time-dependent, behavior is also consistent with the appearance of peaks at the same locations on the reverse scan.

As mentioned above, new anodic peaks appear in the voltage region <3.0 V only after an initial scan to negative bias at a new location. Panels B, C, and D in Figure 8 show three consecutive anodic scans for an acid-promoted SAMs of **V** from 0 to $+3.0$ V at the same spot after a single initial negative tip scan from 0 to -3.0 V (see Figure 8A). All three positive scan curves were recorded at the same tip−substrate distance. For clarity, we show only the forward scans of the $i-V$ curves. In the first positive scan, some fraction ($\sim$25%) of the charge passed in the negative bias regime was recovered at positive tip potentials between 2 and 2.8 V. No significant current flow was observed in the same voltage range in the two subsequent scans. Moreover, no significant current beyond the background noise in the voltage region <2.8 V was observed for an initial positive scan at a new location. These results indicate that about 25% of the charge passed in the negative tip bias regime was

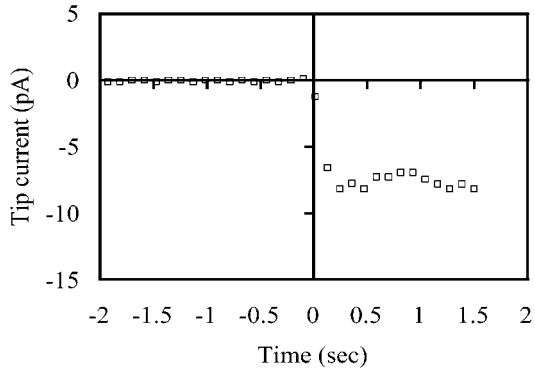

Figure 7. One typical histogram of the current at a tip bias of −2.8 V for a base-promoted SAM of compound **V**. The tip was held at a constant distance from the substrate surface. Current was monitored before the potential was stepped to −2.8 V (at time zero).

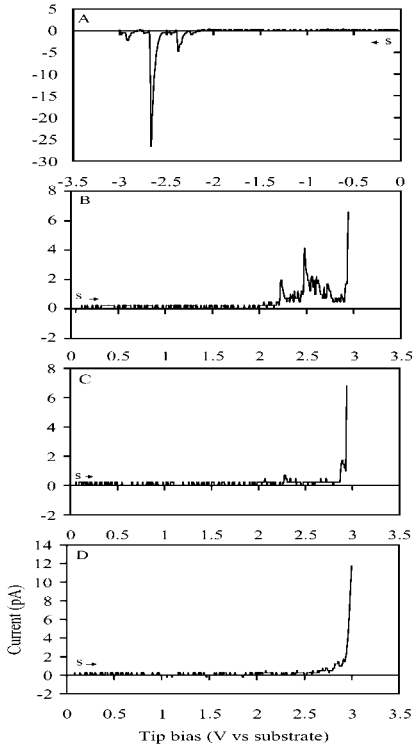

Figure 8. (A) One $i-V$ curve for an initial negative tip scan from 0 to −3.0 V for an acid-promoted SAM of compound **V** (for clarity, only the reverse scan is shown). (B, C, and D) Three consecutive positive scans from 0 to +3.0 V after the initial negative scan A (for clarity, only forward scans are shown).

stored in the molecular layer and could be recovered by biasing the tip at a positive potential. The rest of the charges observed in the negative scan were mainly associated with the resonant tunneling process, as mentioned above. The charge stored in this SAM under the experimental condition for Figure 8, estimated from the current−time relation, was ∼ 90 fC. This corresponds to $\sim 5.6 \times 10^5$ electronic charges or the same number of molecules if we assume each molecule can store one electron. If we take 0.65 nm as the van der Waals diameter of compound **V** and assume that the molecules are closely packed, such number of molecules will cover an area of $\sim 1.8 \times 10^5$ nm^2 or a circular area of diameter $\sim 4.8 \times 10^2$ nm. This number is clearly much larger than the number of molecules in direct contact with the tip. Such an "electrochemical" charge storage process may be of interest in molecular memory devices;[34] however, its detailed mechanism and kinetics need to be investigated further.

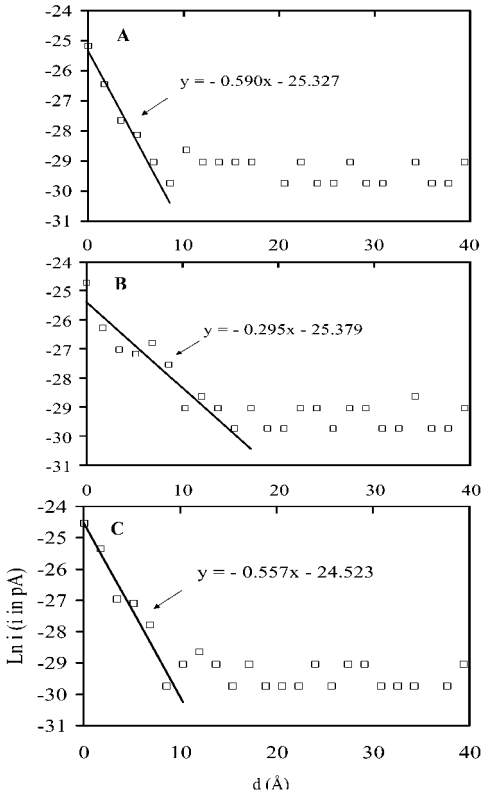

Figure 9. The current vs distance curves at three different tip voltages on a natural logarithmic scale against the tip displacement for SAM of compound **X** on Au: (A) tip bias at −1.0 V; (B) tip bias at −2.5 V; and (C) tip bias at −4.5 V.

Distance Dependence of Film Conductance at Different Bias Voltage. We also explored the current as a function of tip/Au substrate distance at a fixed bias. Figure 9 shows a plot of the current at three different tip voltages on a logarithmic scale vs tip displacement for a SAM of compound **X** on Au. For all three tip-bias values shown in this figure, when the tip was not in contact with the surface of the SAM, no current in excess of the noise was detected. As soon as the tip touched the surface of the SAM, the current increased with decreasing gap, d, between tip and Au substrate according to the empirical relation

$$i = i_0 \exp(-\beta d) \qquad (4)$$

From the slopes of the plots, we obtained the values of β for the three different tip voltages. Clearly the β values for this compound, which shows a cathodic peak during an $i-V$ scan, depend strongly on the tip bias. Figure 10A summarizes the β values of **X** over a tip bias range of −1 to −4.5 V. They range from 0.53 Å^{-1} at −1.0 V to 0.23 Å^{-1} at −3.0 V tip bias.

Panels B and C in Figure 10 summarize the β values of hexadecanethiol, **I**, over a tip bias range of −2.0 to −5.0 V and those of **V** over the range −1.4 to −3.5 V, respectively. These plots show that the β values for **I** were high and did not change significantly over a wide range of tip bias, as previously reported.[19,20,21,24] At voltages near its breakdown voltage (ca.

(34) Reed, M. A.; Chen, J.; Rawlett, A. M.; Price, D. W.; Tour, J. M. *Appl. Phys. Lett.* **2001**, *78*, 3735.

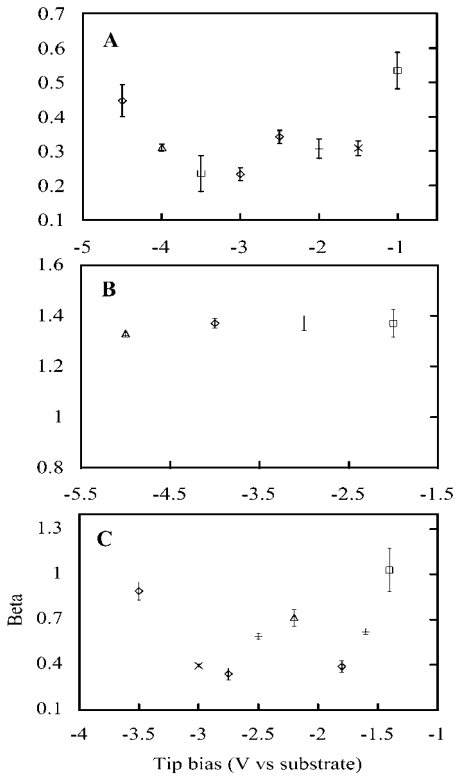

Figure 10. The β values of three compounds as a function of tip bias: curve A for **X**, curve B for **I**, and curve C for **V**.

Table 2. Attenuation Factor, β, and Effective Barrier Height, W_{Eff}, of Various SAMs at −3.0 V Tip Bias (with respect to gold substrate)[a]

compd	β, Å^{-1}	W_{eff}, eV
I	1.37 ± 0.03	1.80 ± 0.09
IV	0.45 ± 0.07	0.19 ± 0.06
V	0.34 ± 0.03	0.11 ± 0.02
VI	0.50 ± 0.05	0.24 ± 0.04
VII	0.15 ± 0.04	0.02 ± 0.01
X	0.23 ± 0.02	0.05 ± 0.01

[a] β and W_{eff} are taken as the average of 10 to 25 curves for each compound at different tip bias (standard deviation shown)

−5.0 V), the β value decreased slightly to ~1.2 Å^{-1}. The values of β for **V** and **X** were structured and changed significantly with tip bias. Of particular interest, both **V** and **X** show the lowest β values within the voltage range where the molecules showed the peaks or highest conductance in the $i-V$ curves.

In Table 2, we summarize the β values and the effective barrier height, W_{eff}, for the different SAMs at a tip bias of −3.0 V. W_{eff} is related to β through eq 5 . Here we assume the Gamow

$$\beta = (4\pi/h)(2mW_{eff})^{1/2} \quad (5)$$

formula (eq 3) is operationally valid, although the physical interpretation of β and W_{eff} is still rather unclear for most of the cases studied here. They seem to provide some information about the relation between molecular electrical property and structure. A theoretical model that incorporates molecular electronic structure into the injection barrier should be helpful for the interpretation of β values. Note that for a series of nitro-based thiol-linked SAMs having the same OPE backbone, W_{eff} and β decrease with an increasing number of nitro groups. Between the two dinitro compounds listed in Table 2, the one having an OPE backbone, **V**, has a lower β and W_{eff} than the one having an OP backbone, **VI**.

Discussion

Electron transport across metal−SAM−metal junctions depends strongly on the position of the Fermi level of the metal electrodes relative to the lowest unoccupied molecular orbital (LUMO) and the highest occupied molecular orbital (HOMO) of the molecular bridge. When the difference in energy between the LUMO and the Fermi level is large, electron transport occurs by superexchange tunneling,[13] i.e., tunneling mediated by interaction between donor and acceptor and unoccupied orbitals of the organic bridge separating them. The $i-V$ characteristics of hexadecanethiol in the low bias regime apparently belong to this category, which shows an exponential increase in current with decreasing distance and has a relatively large β value.[35] If the Fermi level approaches the energy of the molecular orbitals of the molecular bridge, resonant electron transfer may take place and the conduction of electron will occur through the molecular orbitals (MOs), which are affected by interaction with the contacts and by the applied voltage.[13,36] In this case, the current is less distance-dependent and the β value is low and depends strongly on the molecular structure, as observed for most nitro-containing SAMs reported here. There are extensive literature discussions of superexchange tunneling, so we will focus on the resonance tunneling case in the following discussion.

(a) Molecular Orbitals and the Nature of the Interfacial Electronic Structure: A Peak-Shaped $I-V$ Curve. Making electronic contact to molecules is critical in both conventional and single molecule devices. In organic LEDs and FETs, the nature of the charge injection process is an important issue. Interfacial energetics needs to be considered. In the single-molecule device case, it is generally accepted that an MO favorable for conduction requires it to be delocalized while connecting the molecule to the contact electrodes at both ends. The orbitals may be affected by an external electric field or by the state of charge of the molecule.[36] For example, delocalized orbitals can become localized when the molecule traps one electron. Analogously, localized orbitals can become delocalized on an electron transfer. The molecule is in a conducting state if delocalized orbitals are available in the energy range for which one contact has occupied levels and the other has unoccupied ones. The molecule is in a nonconducting state if those orbitals are localized, i.e., both ends of the molecule behave as an insulating layer to the contacts even when the molecular backbone itself is delocalized. According to Seminario's[37] theoretical analysis of metal−molecule contacts, the S−Au interface provides a particularly poor characteristic, which can be considered "insulating" for electron transport through a SAM. It is not unreasonable to treat the (tip/SAM) interface as a blocking layer for electron transport under normal experimental conditions, if there is no strong overlap between the wave functions of tip and SAM. Hence, the present experimental architecture can be considered as consisting of a central quantum well (characterized by discrete electronic levels) separated from

(35) McConnell, H. M. *J. Chem. Phys.* **1961**, *35*, 508.
(36) Seminario, J. M.; Zacarias, A.; Tour, J. M. *J. Am. Chem. Soc.* **2000**, *122*, 3015.
(37) Seminario, J. M.; De La Cruz, C. E.; Derosa, P. A. *J. Am. Chem. Soc.* **2001**, *123*, 5616.

two metallic leads by two thin "insulating" barriers. This is a molecular analogue of the semiconductor resonance tunneling (RT) device. Under such conditions, there is no connection of the LUMO of the molecule with the two terminals. As expected and also observed experimentally, there is a negligibly small current flow in the low bias regime, probably due to the mismatch of the Fermi energy of one electrode with the energy level of the molecular bridge. A very sharp increase in current takes place under the application of a driving voltage where matching the Fermi energy of one electrode to the energy of a discrete electronic level of the quantum well occurs, thus inducing a resonance process across the barriers. One may observe a current peak, if the sharp STM tip has a narrow density of states around the Fermi edge as compared with a bulk electrode, as is usually assumed in the theory of STM.

Furthermore, interfacial energetics is not the only factor to consider in charge injection. Both electronic coupling and charge and nuclear-coordinate relaxation dynamics are important for charge injection at the interfaces. When an electron passes through a molecule, the strong electric field effect may lead to formation of a molecular polaron[38] or a stable anion when a strong electron-accepting group is present. Thus, delocalized orbitals become localized. This might preclude further electron transport based on the theoretical criteria for electron conduction. Even after the decay of the molecular polaron or radical anion, the resulting excitation in nuclear coordinates, and environmental and thermal fluctuations may lead to a metastable structural or conformational change[39] that can lead to the switching behavior and sharp peak current profiles. We use this sharp current peak profile to define the first negative threshold tip bias for resonant conduction, V_{TH}, which is apparently related to the LUMO energy level.

(b) Effect of Molecular Wire Backbone, Electroactive Substituents on Central Benzene Ring, Headgroup at the (Tip/SAM) Interface, and Anchoring Group at the (SAM/Au) Interface. The effective barrier height, as described above, indicates that a dinitro-based thiol-linked SAM having an OPE backbone has lower β and W_{eff} values compared with the same compound having an OP backbone. This is probably due to the conformational twisting of the biphenyls in OP relative to the aryl−alkyne−aryl OPE system. Moreover, the alkynes permit significant overlap of the π-orbital system even with small distortions from planarity and thus increase the delocalization of the MOs, which will decrease the first negative V_{TH}, as experimentally observed. The planarity of the OPEs might also lead to better packing in the self-assembled layer compared to the OP systems.

The effect of electroactive substituents on the central benzene ring on the electric behavior of nitro-containing SAMs is demonstrated by the decrease of the first negative V_{TH} with an increasing number of nitro groups on the central benzene rings. For example, as shown in Table 1, $-V_{TH}$(**II**) > (**III**) > (**V**) ≥ (**VII**) for the first negative threshold voltage. The implication of this finding is that an increase in the number of electron-accepting groups effectively lowers the energy of the LUMO and thus reduces its effective barrier height for electron injection and perhaps also the HOMO-LUMO gap (HLG) of the molecule.

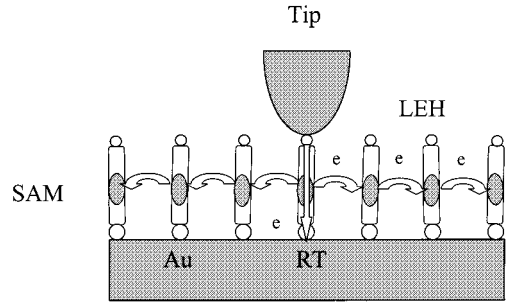

Figure 11. Schematic representation of resonant tunneling (RT, represented as a straight arrow) and lateral electron hopping (LEH, represented as curved arrows) in a MIM junction with a STM tip containing a SAM on Au. The shaded area in the middle zone of the molecules (represented as rods) symbolizes the electroactive groups on the molecule.

Scheme 1

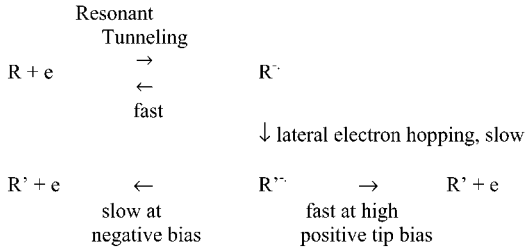

The effect of the headgroup at the (tip/SAM) interface on the performance of the device is quite subtle. For example, the introduction of either a methyl or a COO^- headgroup to a nitro-based compound, **X** or **IX**, is unfavorable for electron injection. Both shift the first negative V_{TH} to more negative values as compared to an H atom, perhaps due to the blocking and electrostatic effects on the interfacial energetics for electron transfer. In terms of the effect of anchoring group at the (SAM/Au) interface on the electric behavior of nitro-based SAMs, a gold−aryl linkage appears to show a smaller barrier for interfacial electron transfer as compared with a gold−sulfur bond. However, unlike the gold−sulfur bond, the identity of the gold−aryl linkage is still unclear and further characterization is needed. Although the thiolate−gold linkage has a higher barrier for electron injection as compared to an aryl−gold linkage, it may not impose a serious problem for electron flow from tip to the substrate. Actually, the easy formation of a high-quality thiol−metal contact has made SAMs of thiols an attractive method for the construction and testing of molecular electronic devices and ready electron transfer to electroactive groups linked to SAMs has been widely observed.[9]

(c) Charge Storage and the Possibility of Lateral Electron Hopping. As mentioned above, we observed, in many cases, anodic peaks appear after the scan of tip potential to negative bias, but an initial scan to positive tip bias at a fresh location did not show a peak in the same positive voltage range. This result is difficult to rationalize based on a pure RT mechanism. However, it is understandable if an electron transfer process occurred laterally near the tip (electron hopping) as shown in Scheme 1 and Figure 11.

Here R and R′ represent neighboring molecules in a nitro-based SAM in the vicinity of the tip, and $R^{-\bullet}$ and $R'^{-\bullet}$ are their radical anions, respectively. As shown in Scheme 1, at V_{TH},

(38) Silinsh, E. A.; Capek, V. *Organic Molecular Crystals: interaction, localization, and transport phenomena;* AIP Press: Woodbury, 1994.
(39) (a) Bumm, L. A.; Arnold, J. J.; Cygan, M. T.; Dunbar, T. D.; Burgin, T. P.; Jones, L., II; Allara, D. L.; Tour, J. M.; Weiss, P. S. *Science* **1996**, *271*, 1705. (b) Donhauser, Z. J.; Mantooth, B. A.; Kelly, K. F.; Bumm, L. A.; Monnell, J. D.; Stapleton, J. J.; Price, D. W., Jr.; Rawlett, A. M.; Allara, D. L.; Tour, J. M.; Weiss, P. S. *Science* **2001**, *292*, 2303.

fast RT takes place at the tip while slow lateral electron hopping occurs in the vicinity of the tip. Lateral electron hopping is slower than RT, since there is little overlap of the wave functions between neighboring molecules and also the field strength parallel to the plane of the substrate in the gap is much weaker than that along the tip−substrate axis. $R'^{-\bullet}$ is stable in the negative tip bias regime and the weak field strength normal to the substrate surface outside the gap. The absence of cations to compensate the charge probably leads to even more effective migration of charge away from the tip area. Hence, at V_{TH} electrons can be stored in the molecules in the vicinity of the tip, until a large positive bias is applied to the tip, where the field is in the direction to bring electrons back to the tip. This model also explains the large amount of stored charge compared to the molecules addressed directly by the tip and suggests the lateral resolution of charge storage in the film may be governed by the field and the migration of charge away from the tip. This model can be tested by SAMs in which the nitro molecules are dispersed in a much larger number of alkane thiols and experiments of this type are contemplated.

Conclusions

Shear force-based SPMs combined with current−voltage and current−distance measurements have been used to probe interfacial electronic structures, particularly unoccupied states, of SAMs of thiolates or arylates on Au. The $i-V$ characteristics of hexadecanethiol in the low bias regime apparently followed the superexchange tunneling mechanism, which showed an exponential increase in current with decreasing distance and were characterized by a relatively large attenuation factor (β value). The β values were nearly independent of tip bias in the range of −2 to −5 V. At ca. −4.95 V, we observed an irreversible negative peak that was not seen in the reverse scan, nor was current detected in a following positive scan, indicating the occurrence of electric breakdown. Different than hexadecanethiol, reversible peak-shaped $i-V$ characteristics were often obtained for most of the nitro-based SAMs studied here, indicating that part of the conduction mechanism for these molecules involves resonance tunneling. These reversible peaked $i-V$ curves manifest the NDR effect of these junctions. Moreover, these nitro-based molecular devices have low β values, ranging from 0.15 $Å^{-1}$ for **VII** and 0.50 $Å^{-1}$ for **VI** at a −3.0 V tip bias. Unlike the β value of hexadecanthiol, these β values depended strongly on the applied voltage. As experimentally observed, they also depend on the structures of the molecules, i.e., electroactive substituent groups on the central benzene ring and their number, the molecular wire backbone, and the anchoring linkage and headgroup. They may also be affected by thermal and environmental factors (e.g., the tip contact pressure as recently proposed by Gimzewski and coworkers and by Son et al.[40]). All of these factors need to be explored further. Another important observable is the threshold voltage for resonant conduction, V_{TH}. Again, the first negative V_{TH} depends strongly on the molecular structure. It ranges from ca. −1.58 V for the quinone compound, **XII**, to ca. −2.8 V for the molecular wire, **II**. These V_{TH} values perhaps reflect the energy of the LUMO of the molecule.

We also observed charge storage with the nitro-based molecules. For the dinitro SAM, ∼25% of charge collected in the negative scan was stored in the molecules and can be read out at positive voltages. The remaining 75% of the total charge represents resonance conduction through the molecule. We propose a mechanism involving lateral electron hopping to explain this phenomenon. The implication of this finding is that charging a SAM that simultaneously has one or more conduction channels requires that the anions are dynamic species having sufficiently long electron retention times. Elucidation of the detailed mechanisms and kinetics is certainly important for potential application and requires further investigation.

Acknowledgment. We would like to acknowledge support of this research by the Robert A. Welch Foundation, the National Science Foundation (CHE-0109587), and the Laboratory of Electrochemistry Organized Research Unit. J.M.T. thanks the Defense Advanced Research Projects Agency via the Office of Naval Research, and Molecular Electronics Corp. for support.

JA017706T

(40) See, e.g.: (a) Joachim, C.; Gimzewski, J. K *Proc. IEEE* **1998**, *86*, 184. (b) Son, K. A.; Kim, H. I.; Houston, J. E. *Phys. Rev. Lett.* **2001**, *86*, 5357.